

# TAPER SHAPES DESIGN CHARTS FOR KLOPFENSTEIN AND HECKEN TYPE MICROSTRIP LINE TAPERS BY MODE-MATCHING and FDTD TECHNIQUES.

Hirokimi Shirasaki

Tamagawa University, Electrical Engineering Dept., 6-1-1 Tamagawa-Gakuen, Machida, Tokyo 194-8610, Japan

E-mail: [shira@eng.tamagawa.ac.jp](mailto:shira@eng.tamagawa.ac.jp)

## ABSTRACT

The optimum shapes in which the reflected wave decreases at a specific frequency for a satellite broadcast reception were considered with the Klopfenstein and Hecken tapers. The scattering coefficients were obtained by using both the mode-matching and generalizing scattering methods. The  $\lambda/4$  transformer changes to the Klopfenstein tapers, and the exponential taper changes to the Hecken tapers, when a longer length is used in the wide passband frequency. Then, the practical design charts for optimum taper shapes were obtained. Finally, the scattering coefficients for the optimum taper shapes are analyzed by FDTD methods to analyze the effect of radiation.

## INTRODUCTION

The optimum shapes in which the reflected wave decreases at a specific frequency for a satellite broadcast reception were then considered with the Klopfenstein and Hecken tapers in Refs. [1]. The tapered parts were divided like a flight of stairs. The scattering coefficients of each step were combined by using both the mode-matching and generalizing scattering methods [2]. The  $\lambda/4$  transformer changes to the Klopfenstein taper shapes, and the exponential taper changes to the Hecken taper shapes, when a longer length is used in the wide passband frequency. By choosing the parameters adequately, it becomes possible to choose the appropriate proportioned necessary bandwidths. In this paper, practical designs for optimum shapes are obtained using the Klopfenstein and Hecken tapers when the reflected wave decreases at a specific frequency for the satellite broadcast reception. When the taper length is shorter than a half lambda, the effect of radiation has to be analyzed. Then, the taper shapes are analyzed by the FDTD method. The Hecken taper reflection coefficients which are longer than a half lambda by the FDTD method are similar to those of the mode-matching method. The Klopfenstein taper reflection coefficients which are less than a half lambda by the FDTD method are slightly different from those of the mode-matching method.

## MODE-MATCHING ANALYSIS

### Waveguide Model

The characteristic impedances of the input part and the output part of the microstrip line are assumed to be  $Z_a$  and  $Z_b$ . The envelope of the characteristic impedance of each step in the tapered part, changes gradually which is assumed for  $N-1$  to be divided at equal intervals, change as follows [3][4];

$$\text{Klopfenstein taper: } Z_m = \exp[\ln(Z_a Z_b)/2 + \Gamma_0 A^2 \phi(2m/N - 1, A) / \cosh(A)] \quad (1)$$

$$\text{Hecken taper: } Z_m = \exp[\ln(Z_b Z_a)/2 + \gamma_0 B \phi(2m/N - 1, B) / \sinh(B)] \quad (2)$$

$$\text{where, } \Gamma_0 = (Z_b - Z_a)/(Z_b + Z_a), \quad \gamma_0 = \ln(Z_b / Z_a) / 2 \quad (3)$$

$$\phi(x, A) = \int_0^x I_1(A\sqrt{1-y^2}) / (A\sqrt{1-y^2}) dy, \quad \phi(x, B) = \int_0^x I_0(B\sqrt{1-y^2}) dy \quad (4)$$

$N$  is the number of steps. The width of an actual strip line is obtained from this characteristic impedance. The next equation was used as characteristic impedance  $Z_n$  according to Ref. [5];

$$Z_n(u_n, f) = \frac{60}{\sqrt{\epsilon_{re}(u_n, f)}} \ln \left[ \frac{f(u_n)}{u_n} + \sqrt{1 + \left( \frac{2}{u_n} \right)^2} \right], \quad u_n = \frac{W_n}{h} + \Delta u \quad (5)$$

where  $\epsilon_{re}$  is an effective relative permittivity [5],  $f$  is a frequency,  $t$  is the strip thickness,  $h$  is the substrate thickness,  $\epsilon_r$  is the substrates' relative permittivity, and other variables have been shown in Ref. [2][5]. Because the  $Z_n$  is given by the width  $W_n$  from Eq. (5), the  $W_n$  is obtained from the  $Z_n$  numerically. This algorithm is shown in Ref. [5]. Because the  $W_n$  is not uniquely decided if the frequency is not given in this procedure, the frequency  $f_z$  is introduced.

The next equation was used as the effective width [6];

$$W_{e,n}(f) = W_n + \frac{W_{e,n}(0) - W_n}{1 + f/f_n}, \quad W_{e,n}(0) = \sqrt{\frac{\mu_0}{\epsilon_0}} \frac{h}{\sqrt{\epsilon_{re}(u(W_n), 0)}}, \quad f_{g,n} = \frac{1}{2W_n \sqrt{\epsilon_r \epsilon_0 \mu_0}}, \quad (6)$$

where  $\epsilon_0$  and  $\mu_0$  are the permittivity and permeability in the vacuum, respectively. If the effective width and the effective relative permittivity are obtained from the characteristic impedance, it can be analyzed as well as Ref. [2]. The concept of the waveguide model is equal with magnetic walls on both sides and is equal in the effective width  $W_{e,n}$  and the effective relative permittivity  $\epsilon_{re}$ . The substrate's height is assumed to be equal, and neither the radiation wave nor the surface wave are considered.

### Analysis of single step and multi-step connection

Because the analysis of the single step is described in detail in Ref. [2], the procedure of the analysis is explained here. Figure 1 shows a supplementary structure in each stair. The normal modes in each area are  $A_n$  and  $P_n$ . The single step is analyzed by using the mode-matching method and scattering coefficients are obtained by putting  $d=0$  in Fig. 1. Then, the scattering matrix for the multi-step connection is obtained by the generalized scattering matrix method [2]. The transmission matrix in area  $A_n$  is given by

$$\mathbf{T} = \begin{bmatrix} \mathbf{I} & \mathbf{0} \\ \mathbf{0} & \mathbf{T}(L) \end{bmatrix}, \quad T_m(L) = \exp(\gamma_{A_n}^m), \quad m = 1, 2, 3, \dots \quad (7)$$

where  $\mathbf{T}(L)$  is a matrix whose element is given by  $T_m$ . The combined scattering matrix  $\mathbf{S}^{AL}$  is a combination of the scattering matrix  $\mathbf{S}^A$  at the boundary of  $\mathbf{S}^n$ , and the phase change  $\mathbf{T}(L)$  in the length of step  $L$ , is given by,

$$\mathbf{S}^{AL} = \mathbf{T} \mathbf{S}^A \mathbf{T} = \begin{bmatrix} \mathbf{S}_{11} & \mathbf{S}_{12} \mathbf{T}(L) \\ \mathbf{T}(L) \mathbf{S}_{21} & \mathbf{T}(L) \mathbf{S}_{22} \mathbf{T}(L) \end{bmatrix}, \quad (8)$$

The combined scattering matrix  $\mathbf{S}^{AL}$  along with the scattering matrix  $\mathbf{S}^B$  at the boundary of  $\mathbf{S}_{n+1}$ , is given by

$$\begin{aligned} \mathbf{S}_{11} &= \mathbf{S}_{11}^{AL} + \mathbf{S}_{12}^{AL} \mathbf{S}_{11}^B (\mathbf{I} - \mathbf{S}_{12}^{AL} \mathbf{S}_{11}^B)^{-1} \mathbf{S}_{21}^{AL}, & \mathbf{S}_{22} &= \mathbf{S}_{11}^B + \mathbf{S}_{21}^B \mathbf{S}_{11}^{AL} (\mathbf{I} - \mathbf{S}_{12}^{AL} \mathbf{S}_{11}^B)^{-1} \mathbf{S}_{21}^{AL} \mathbf{S}_{12}^B, \\ \mathbf{S}_{21} &= \mathbf{S}_{21}^B (\mathbf{I} - \mathbf{S}_{12}^{AL} \mathbf{S}_{11}^B)^{-1} \mathbf{S}_{21}^{AL}, & \mathbf{S}_{12} &= \mathbf{S}_{12}^{AL} [\mathbf{S}_{11}^B (\mathbf{I} - \mathbf{S}_{12}^{AL} \mathbf{S}_{11}^B)^{-1} \mathbf{S}_{22}^{AL} \mathbf{S}_{11}^B + \mathbf{S}_{12}^B], \end{aligned} \quad (9)$$

It is necessary to repeat this operation for the multi-step process.

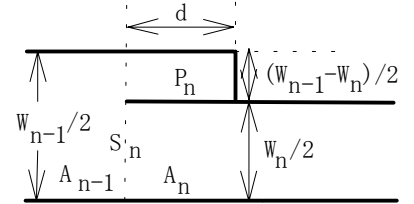


Fig.1 Supplementary structure.

### NUMERICAL CALCULATIONS BY MODE MATCHING METHODS

We calculate the relative permittivity at  $\epsilon_r=1.75$ , the substrate's height is at  $h=1(\text{mm})$ , and the strip thickness is at  $t=35(\mu\text{m})$ . We use 24 sets of modes to calculate the value of the scattering coefficient, and this helped us find the convergence. The numbers of steps  $N$  are equally divided in length by  $L=0.1(\text{mm})$ . For example, it is  $N=50, 100, 150$  for the taper length  $L=5, 10$  and  $15(\text{mm})$ , respectively.

### Impedance shapes of tapers

Figures 2 shows the impedance shapes of tapers which changed from 50  $\Omega$  to 100  $\Omega$ .  $A$  and  $B$  in Figs. 2 are parameters which decide attenuations in the passband. By changing  $A$  and  $B$ , the taper shapes changed. The Klopfenstein taper appears at  $\lambda/4$  transformer so that  $A=0$ . They both have the impedance steps for the input and output parts. In  $B=0.2$ , the shapes of Hecken and exponential tapers almost agree. They are without steps in the input and output parts.

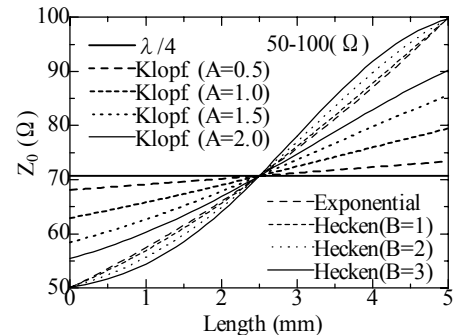


Fig.2 Impedances of Klopfenstein and Hecken taper.

## Reflection properties

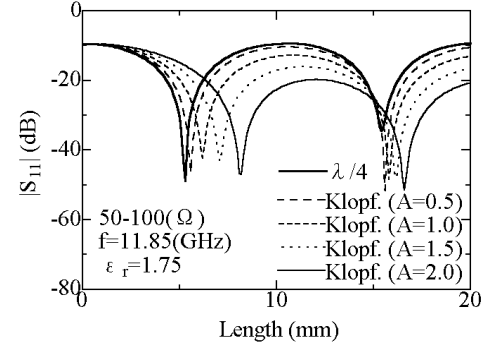
The taper shapes in which the reflection coefficient is minimized at the frequency 11.85GHz are obtained. In Ref. [3][4], the reflection coefficients were obtained by using the approximation method. Here, the numerical calculations have been carried out based on the mode-matching method. In Figs. 3(a) and (b), the reflection characteristics as the taper length changes are shown. At the fixed frequency of 11.85GHz, the reflection coefficient is minimized. On the first fall, the quarter lambda has the shortest taper length. When we increase A, the first fall is lengthened. In B=0.2, the characteristics of Hecken tapers and exponential tapers almost agree. When B is increased, the length of the first reflection fall is lengthened. In Figs. 4(a) and (b), the frequency characteristics of the reflection coefficient at the first reflection fall length in Fig. 2 are shown. It shows that the bandwidth at frequency 11.85(GHz) enlarges as the taper length is lengthened.

## Design charts

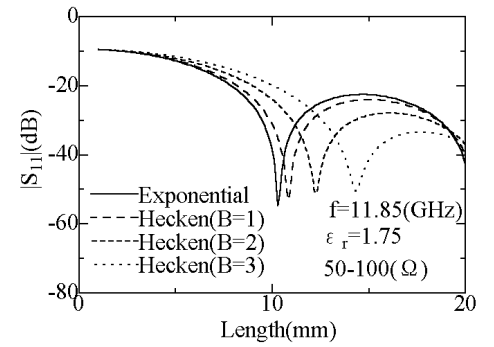
In Figs. 5(a) and (b), the practical design charts for optimum shapes in which the reflected wave decreases at 11.85(GHz) are obtained with Klopfenstein and Hecken tapers. Each vertical axis is the taper length to which the reflection coefficients first fall, and the bandwidth. When the reflection coefficient is -30, -35, and -40(dB), the bandwidth is shown. In Fig. 5(a), the  $\lambda/4$  transformer [A=0: the black dots (the bandwidths) and the white squares (the taper length)] change to the Klopfenstein taper shapes while lengthening the taper length, when using the wide passband. In Fig. 5(b), the exponential taper [B=0: the black dots (the bandwidths) and the white squares (the taper length)] change to the Hecken taper shapes when a lengthened length is used in the wide passband frequency. Therefore, by choosing the parameter A and B adequately in these design charts, it becomes possible to get the optimum taper shape when it is in proportion to the necessary bandwidth.

## FDTD ANALYSIS

When the taper length is shorter than a half lambda, the effect of radiation has to be analyzed. Then, the taper shapes are analyzed by the FDTD method. The FDTD method is to approximate the Maxwell equation by a finite difference and to solve by the time domain [7]. In this method, the analytic region includes a source and scattering fields and is divided by small cells. The analytic model is shown in Fig. 6. The cell sizes are  $\Delta x = \Delta y = \Delta z = 0.05(\mu m)$ . The analytic region sizes are NX=126, NY=229, NZ=600. Because the FDTD method is for closed region problems, the perfectly matching layer (PML) is used as absorbing conditions for open region problems. We obtain the pulse propagation characteristics of the tapers and a 50  $\Omega$  straight line stimulated by Gaussian pulse sources. Then subtracting the taper pulse characteristics from the straight line pulse characteristic and processing by FFT, we obtain the reflection coefficients. Figure 7 shows the comparison between the reflection coefficients of mode matching and FDTD methods. The Hecken taper reflection coefficients which are longer than a half lambda by the FDTD method are similar to those of the mode-matching method and the fall frequencies are 11.85GHz both. The Klopfenstein taper reflection coefficients which are less than a half lambda by the

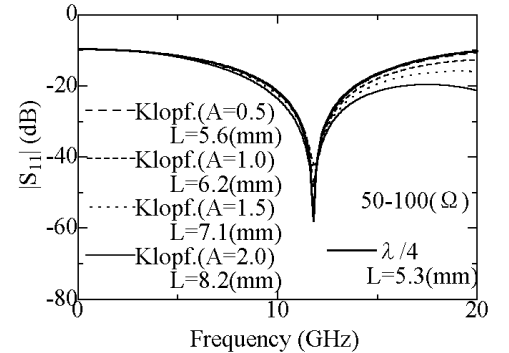


(a) Klopfenstein taper

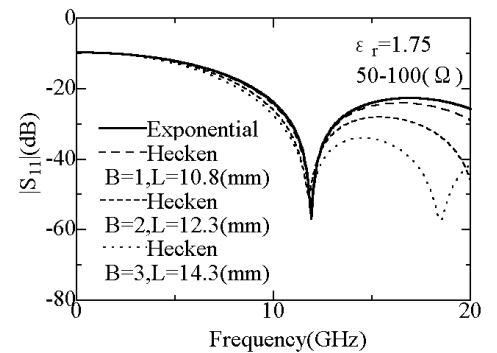


(b) Hecken taper

Fig.3 Reflection characteristics.

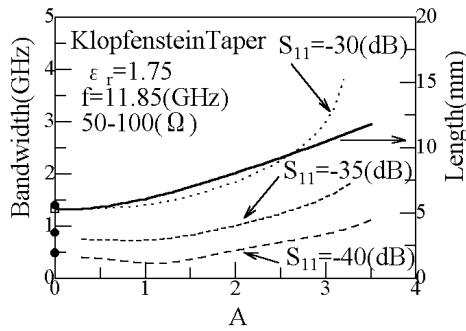


(a) Klopfenstein taper

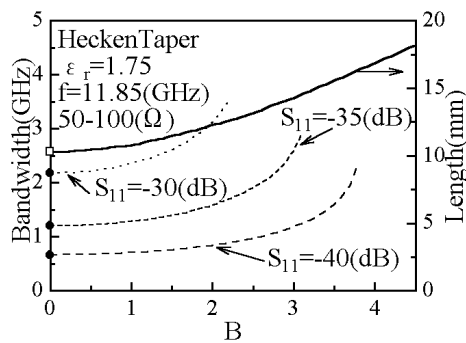


(b) Hecken taper

Fig.4 Reflection characteristics.



(a) Klopfenstein taper



(b) Hecken taper

Fig.5 Design charts.

FDTD method are slightly different. The fall frequency is 11.84GHz by the mode-matching method and is 11.65GHz by the FDTD method. It is considered that the frequency fall points are slightly deferent because the Klopfenstein tapers have the impedance steps for the input and output parts.

## CONCLUSION

The practical design charts for optimum taper shapes were obtained by the mode-matching methods. The rightness of the scattering coefficients for the optimum taper shapes are examined by the FDTD methods. Then, the frequencies at the reflection coefficient fall points are coincidental for the Hecken tapers but are slightly deferent for the Klopfenstein tapers. We will analyze the effect of radiation and other reasons for the slight frequencies' differences later.

## REFERENCES

- [1] H. Shirasaki, "Optimum Design by Waveguide Model and Mode Matching Technique of Microstrip Line Taper Shapes for Satellite Broadcast Planar Antenna", 1999 IEEE AP-S and USNC/URSI, AP-16-065, July 1999.
- [2] H. Shirasaki, "Steps Approximate Analysis of Linear and Raised Cosine Tapered Microstrip Lines by Waveguide Model", IEICE, Vol J79-C-I, No 8, pp 303-309, Aug. 1996.
- [3] R.W. Klopfenstein, "A Transmission Line Taper of Improved Design", Proc. IRE, Vol.44, pp.31-35, 1956.
- [4] R.P. Hecken, "A Near-Optium Matching Section Without Discontinuities", IEEE, Vol MTT-20, pp 734-739, 1972.
- [5] S. Roslonic, "Algorithms for Computer-Aided Design of Linear Microwave Circuits," p 196, Artech House, 1990.
- [6] K. C. Gupta, R. Garg, I. J. Bahl, "Microstrip Lines and Slotlines", p 27, Artech House, 1990.
- [7] A. Taflove and S.C. Hagness: "Computational electrodynamics: The finite-difference time-domain method, " Artech House, 2000.

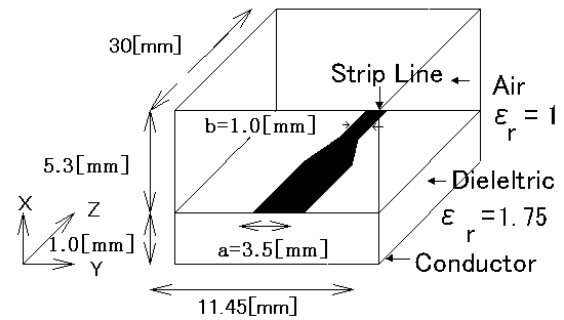
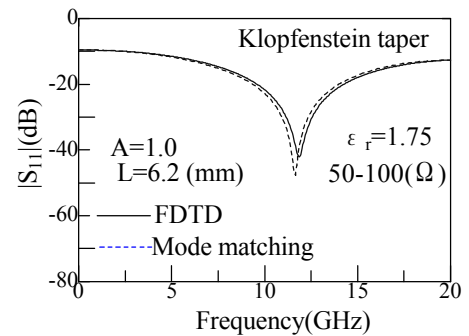
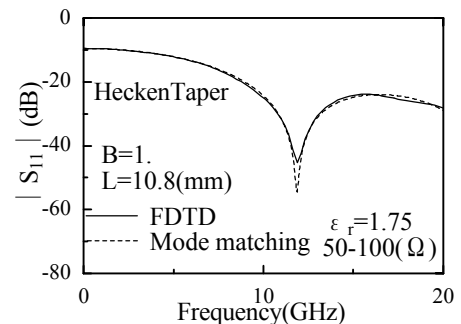


Fig.6 Analytic model.



(a) Klopfenstein taper



(b) Hecken taper

Fig.7 Comparisons of Reflection characteristics.